

A Study of the Asymmetric Wave Parameterize

Yun-Chih Chiang, Sung-Shan Hsiao, Hui-Ming Fang, and Hsing-Yu Wang

Abstract—Coastal sedimentation is a crucial topic in the field of modern coastal engineering. In general, coastal sediment-transport mechanisms are changing because large-scale coastal engineering projects have blocked coastal sediment transport, regional coastal development has destroyed natural protective barriers, and climate changes and global warming have caused sea levels to rise and changed wave flow fields. This study used Stokes 2nd theory as the theoretical basis for nonlinear waves in nearshore non-breaking regions. In addition, in nearshore wave-breaking regions, flow velocity at the bottom approximates sawtooth waves. If the difference in the wave steepness or the water depth parse obtained the surf similarity parameter is larger, the smaller the asymmetry parameter.

Index Terms—Sawtooth waves, surf similarity parameter, asymmetry parameter.

I. INTRODUCTION

The continuity of coastal sand flow may be blocked by artificial structures, giving rise to difficulties for coastal protection during the process of coast reconstruction within a coastal dynamic system. Such system is subjected to the principles of conservation of energy. Littoral drift, known as two-phase flow, is a phenomenon resulted from the interaction between tidal wave flows and the seabed substrate. Analysis of the dynamics of flows and substrate particles is therefore crucial to understanding the mechanism of two-phase flows. As one of the driving forces for seabed sediment drift, breaking waves, when typical and incident, generate underwater countercurrents, causing vertical sand movement offshore; when the waves penetrate at diagonal angles, the breaking waves generate littoral currents, driving flows and sands within the surf zone to move parallel to the shoreline. These tidal wave derived agents are the main driving forces for littoral drift. However, the seabed morphology and shifting effects after the initialization of littoral drifts, and the interaction between drift initialization and wave flows, remain unclear. Consequently, current estimation of sand drift volume is still based on empirical or semiempirical equations.

Given the complexity and irreversibility of the dynamic process of coastal topography, which is subjected to impacts of climate and marine conditions as well as artificial structures, coastal flows and wave propagation caused by

nearshore topographic changes must considered. During wave movements, waves undergo changes in height, wavelength, and waveforms while water depth decreases. When the water depth is reduced to a certain extent, breakers may arise, resulting in littoral currents, which in turn may impact littoral drift and coastal topography. On the basis of the height and period of the incident deep sea waves, and the floor slope, [1] and [2] have categorized breakers into three types, namely spilling breaker, plunging breaker, and surging breaker.

Because the peak amplitude of the waves is greater than their trough amplitude in shallow water, and that the seabed is a slope of a nonfinite length, the velocity of particle transport varies by section and elevation, creating what is known as the asymmetry of waves. By drawing on research findings from related literature for future marine topographical monitoring and reconstruction, this study examined the parameters of agents such as littoral drift and coastal transport mechanics within surf zones. This study anticipated providing a reference for estimating littoral drift trends in practical coastal topography and parameter computation.

II. BASIC ASSUMPTIONS AND THE COORDINATE SYSTEM

A. Control Formula

To compute the hydrodynamic conditions at the surf point of the coast profile, this study employed the Galerkin finite element method to calculate the variable defined in the structural grid by using the Boussinesq equation with improved mixed interpolation, which is used to simulate waves propagating from deep-water toward the shore. The water depth and wavelength ratio (h/L) were required to be less than 0.5. The continuous equation and momentum equation are as shown in Eqs. (1) to (3):

The continuous equation:

$$n \frac{\partial \xi}{\partial t} + \frac{\partial P}{\partial x} + \frac{\partial Q}{\partial y} = 0 \quad (1)$$

The momentum equation on the x direction:

$$n \frac{\partial P}{\partial t} + \frac{\partial}{\partial x} \left(\frac{P^2}{h} \right) + \frac{\partial}{\partial y} \left(\frac{PQ}{h} \right) + \frac{\partial R_{xx}}{\partial x} + \frac{\partial R_{xy}}{\partial x} + n^2 gh \frac{\partial \xi}{\partial x} + n^2 P \left[\alpha + \beta \frac{\sqrt{P^2 + Q^2}}{h} \right] + \frac{gP \sqrt{P^2 + Q^2}}{h^2 C^2} + n \Psi_1 = 0 \quad (2)$$

The momentum equation on the y direction is:

Manuscript received February 15, 2016; revised April 5, 2016.

Yun-Chih Chiang is with the Center for General Education, Tzu Chi University, Hualien, Taiwan (e-mail: ychiang@mail.tcu.edu.tw).

Sung-Shan Hsiao, Hui-Ming Fang, and Hsing-Yu Wang are with the Department of Harbor and River Engineering, National Taiwan Ocean University, Keelung, Taiwan (e-mail: sshsiao@mail.ntou.edu.tw, fred3618@gmail.com, hywang1108@gmail.com).

$$n \frac{\partial Q}{\partial t} + \frac{\partial}{\partial y} \left(\frac{Q^2}{h} \right) + \frac{\partial}{\partial x} \left(\frac{PQ}{h} \right) + \frac{\partial R_{xx}}{\partial x} + \frac{\partial R_{xy}}{\partial x} + n^2 gh \frac{\partial \xi}{\partial x} + n^2 Q \left[\alpha + \beta \frac{\sqrt{P^2 + Q^2}}{h} \right] + \frac{gQ\sqrt{P^2 + Q^2}}{h^2 C^2} + n\Psi_2 = 0 \quad (3)$$

Here, discret factors Ψ_1 and Ψ_2 are:

$$\Psi_1 = - \left(B + \frac{1}{3} \right) d^2 (P_{xxt} + Q_{xyt}) - nBgd^3 (\xi_{xxx} + \xi_{xyy}) - dd_x \left(\frac{1}{3} P_{xt} + \frac{1}{6} Q_{yt} + nBgd (2\xi_{xx} + \xi_{yy}) \right) - dd_y \left(\frac{1}{6} Q_{xt} + nBgd \xi_{xy} \right) \quad (4)$$

$$\Psi_2 = - \left(B + \frac{1}{3} \right) d^2 (Q_{yyt} + P_{xyt}) - nBgd^3 (\xi_{yyy} + \xi_{xxy}) - dd_y \left(\frac{1}{3} Q_{yt} + \frac{1}{6} P_{xt} + nBgd (2\xi_{yy} + \xi_{xx}) \right) - dd_x \left(\frac{1}{6} P_{yt} + nBgd \xi_{xy} \right) \quad (5)$$

The horizontal direction of the pressure gradient relationship, such as Eqs. (6) and (7):

$$F_x = - \left(\frac{\partial}{\partial x} \left(v_t \frac{\partial P}{\partial x} \right) + \frac{\partial}{\partial y} \left(v_t \left(\frac{\partial P}{\partial y} + \frac{\partial Q}{\partial x} \right) \right) \right) \quad (6)$$

$$F_y = - \left(\frac{\partial}{\partial y} \left(v_t \frac{\partial Q}{\partial y} \right) + \frac{\partial}{\partial x} \left(v_t \left(\frac{\partial Q}{\partial x} + \frac{\partial P}{\partial y} \right) \right) \right) \quad (7)$$

In addition, this study in order to obtain the hydrodynamic conditions on the coast sectional of introducing the Eqs. (8) which auxiliary variables displayed, and into the higher-order derivatives terms, instead of lower-order, such as shown in Eqs. (9) and (10). After due consideration of the spatial derivative of the Second Order, and was replaced with standard Galerkin finite element method, discrete items using Boussinesq divergence theorem, this equation can be inserted within the functional form of continuous performance. Therefore, the auxiliary variables are:

$$w = \frac{\partial}{\partial x} \left(d \frac{\partial \xi}{\partial x} \right) \quad (8)$$

The continuous equation is

$$n \frac{\partial \xi}{\partial t} + \frac{\partial P}{\partial x} = 0 \quad (9)$$

And the momentum equation is

$$n \frac{\partial P}{\partial t} + \frac{\partial}{\partial x} \left(\frac{P^2}{h} \right) + \frac{\partial R_{xx}}{\partial x} + n^2 gh \frac{\partial \xi}{\partial x} - n \left(B + \frac{1}{3} \right) d^2 \frac{\partial^3 P}{\partial x \partial x \partial t} + \frac{1}{3} d \frac{\partial d}{\partial x} \frac{\partial^2 P}{\partial x \partial t} - n^2 Bgd^2 \frac{\partial w}{\partial x} + n^2 P \left[\alpha + \beta \frac{|P|}{h} \right] + \frac{gP|P|}{h^2 C^2} = 0 \quad (10)$$

B. Breaker Index

In general, breaker indices can be expressed using parameters of water depth at the breaking point, wave height, and cycle. Alternatively, they can be expressed using parameters of deep sea wave height and cycles. Previous studies have noted that breaker indices are related to seabed slope. The [3] proposed an approximate expression as shown in Eq. (11)

$$\frac{H_b}{L_0} = 0.17 \left\{ 1 - \exp \left[-1.5 \frac{\pi h_b}{L_0} (1 + 15m^{4/3}) \right] \right\} \quad (11)$$

The [4] proposed a breaker index equation as is shown in Eq. (12)

$$\frac{H_b}{L_b} = 0.14 \tanh \left[(0.8 + 5m) \frac{2\pi h_b}{L_b} \right] \quad m < 0.1$$

$$\frac{H_b}{L_b} = 0.14 \tanh \left[(1.3) \frac{2\pi h_b}{L_b} \right] \quad m > 0.1 \quad (12)$$

The [5] introduced a simplified empirical equation as is shown in Eq. (13)

$$\frac{H_b}{h_b} = 1.09m^{0.19} \left(\frac{h_b}{L_0} \right)^{-0.1} \quad (13)$$

Considering the effect of floor slope, [5] and [6] have observed the relationships between wave height, offshore wave steepness, and seabed slope, and have expressed this relationship in Eqs. (14) and (15), respectively:

$$\frac{H_b}{H_0} = 0.76(m)^{1/7} \left(\frac{H_0}{L_0} \right)^{-0.25} \quad (14)$$

$$\frac{H_b}{H_0} = (m)^{0.2} \left(\frac{H_0}{L_0} \right)^{-0.25} \quad (15)$$

To determine the water depth and height of breaking waves, this study used the breaker indices introduced by [3], which are commonly used in coastal engineering worldwide and in Eq. (11). Combined with Eq. (14), which was introduced by [6] for estimating the relationship between wave height, offshore wave steepness, and bottom slope, the relationships between water depth at the surf point, deep sea wave steepness, and floor slope can be expressed as Eq. (16):

$$\frac{h_b}{L_0} = \frac{\ln \left[1 - 4.47(m)^{1/7} \left(\frac{H_0}{L_0} \right)^{0.75} \right]}{1.5\pi (1 + 15m^{4/3})} \quad (16)$$

III. ASYMMETRIC WAVE ANALYSIS

A. Basic Assumptions

Based on the [7] and [8] transmission of sequential waves

toward the coast, the time-dependent velocity of one wave period (T) near the seabed was calculated and is shown in Fig. 1. The wave period and its velocity near the seabed are divided into positive and negative half-cycles T_c and T_t ; c represents the crest half-cycle, and t represents the trough half-cycle. Therefore, $T=T_c+T_t$. The highest amplitude wave half-cycle is denoted by u_{max} ; the time between zero and the upper tangent is denoted by T_{pc} ; the difference between the highest flow and lowest flow speed in the wave period is denoted by \hat{u} ; and the time between zero and the lower tangent in the negative flow speed half-cycle is denoted by T_{pt} . Among these variables, u represents periodic velocity components and steady flow.

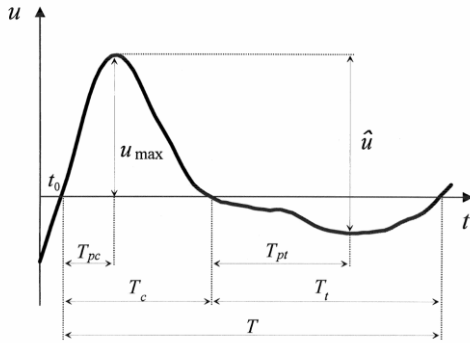


Fig. 1. Time-dependent velocity of one wave period near the seabed [9].

Because [7] and [8] based their results of the phenomenon and the coefficients of asymmetric wave model theory on observational data, they are usable only under certain conditions. To broaden the applicability of the overall sediment formula, nonlinear wave theory was incorporated and analyzed. [8] performed a series of observations and defined the following asymmetric wave variables: amplitude of wave trajectory and velocity (U_w); the ratio between the highest flow rate in a crest half-cycle and the difference between the highest and lowest flow rates in a wave period (u_{max} / \hat{u}); the appearance time of the highest dimensionless flow rate ($2T_{pc}/T$); and the flow speed of a steady flow (U_0). By using nonlinear wave theory, the primary observed asymmetrical parameters can be solved theoretically, and can be directly applied to an appropriate sediment-rate formula for analysis. These nonlinear wave theories are each applicable to different water depths. However, using multiple nonlinear wave theories to describe sediment-transport rate models, which must be developed from coastal landform-change models, increases complexity.

Water particle velocity:

$$u = \frac{\pi H}{T} \frac{\cosh k(z+h)}{\cosh kh} \cos(kx - \sigma t) \quad (17)$$

$$w = \frac{\pi H}{T} \frac{\sinh k(z+h)}{\cosh kh} \sin(kx - \sigma t) \quad (18)$$

Maximum water particle velocity:

$$u_{max} = \frac{\pi H}{T} \frac{\cosh k(z+h)}{\cosh kh} \quad (19)$$

$$w_{max} = \frac{\pi H}{T} \frac{\sinh k(z+h)}{\cosh kh} \quad (20)$$

B. Current Velocity Analysis

To obtain the velocity near the sea bed, this study followed the suggestion by [9] and used Stokes 2nd theory as the theoretical basis for nonlinear waves in nearshore non-breaking regions. Stokes 2nd theory can be applied to entire nearshore regions; although flow velocity at the bottom can be over or underestimated, the error margins of average wave velocity are within an acceptable range. In addition, in nearshore wave-breaking regions, flow velocity at the bottom approximates sawtooth waves. Using Stokes 2nd theory ([10]), the bottom trajectory velocity can be expressed as:

$$u_w(t) = U_w \left(\cos(\omega t) + \frac{3kH}{8\sinh^3(kh)} \cos(2\omega t) \right) \quad (21)$$

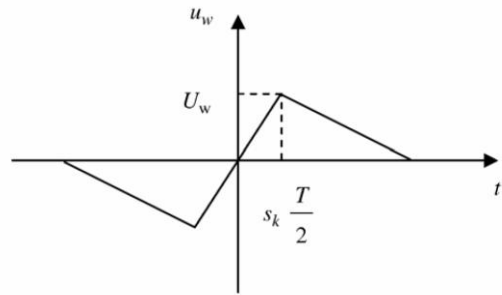


Fig. 2. Sawtooth wave time-dependent velocity.

Although inconsistencies remain in this theory ([11]), the calculations are convenient to use and the error margins are within an acceptable range. Therefore, sawtooth wave theory was adopted in this study to explore the time-dependent velocity distribution of asymmetrical flow velocities in wave-breaking regions. Time-dependent flow velocity in the breaking region can be described using sawtooth waves (Fig. 2),

$$u_w(t) = U_w f(t) \quad (22)$$

where U_w represents the velocity amplitude of linear seabed waves, H denotes the ripple height, h represents the water depth, and k denotes the ripple number. After obtaining the dispersion relationship $\omega^2 = gk \tanh(kh)$, the result is $U_w = \omega h / (2 \sinh(kh))$.

$$U_w = \frac{\omega h}{(2 \sinh(kh))} \quad (23)$$

And in equation (22):

$$f(t) = \begin{cases} \frac{2t}{s_k T}, & t \leq \frac{s_k T}{2} \\ \frac{T-2t}{(1-s_k)T}, & \frac{s_k T}{2} \leq t \leq \frac{T}{2} \end{cases} \quad (24)$$

Asymmetrical parameter coefficient s_k in Eq. (24) can be expressed as follows: $s_k = \frac{T_{pc}}{T_c}$.

Therefore, the root mean square of the velocity of the wave trajectory is

$$u_{rms}^2 = \frac{U_w^2}{3} \quad (25)$$

The velocity components of waves in crest and trough half-cycles on the x -axis are

$$u_{cx}^2 = U_w^2 \times \frac{2}{3} (1 + r_{cw})^2 \quad (26)$$

$$u_{tx}^2 = U_w^2 \times \frac{2}{3} (1 - r_{cw})^2 \quad (27)$$

The dimensionless crest and trough half-cycles are

$$(t_c, t_t) = \left(\frac{T_c}{T}, \frac{T_t}{T} \right) = \left(\frac{1}{2} (1 + r_{cw}), \frac{1}{2} (1 - r_{cw}) \right) \quad (28)$$

IV. COMPREHENSIVE DISCUSSION

In order to calculate the hydrodynamic conditions on the coast sectional wave breaking point, this study uses Galerkin finite element method, it is definitions of the variable structure of the grid in the mix for solving differential to calculate the improvement Boussinesq equations, and the input data shown in Table I. Since the coastal wave breaking caused by current changes may affect the coastal sediment transport and terrain changes, so by different deep-sea incident height, period, and the bed slope, [12] proposed surf similarity parameter, aimed at determining the type of wave breaking. Different types of wave breaking are shown in the Table II. In this study, in order to simplify the subsequent solving, using deep sea in this incident conditions is calculated:

$$\xi_0 = \frac{m}{\sqrt{H_0 / L_0}} \quad (29)$$

$$\xi_b = \frac{m}{\sqrt{H_b / L_b}} \quad (30)$$

By substituting Eq. (29) and Fig. 3, the surf similarity parameter indicators related primarily to breaker index:

$$\frac{H_0}{L_0} = m(\xi_0)^{-0.5} \quad (31)$$

This study followed [8] stokes second-order theory as the theoretical basis to examine nearshore seabed current velocity distribution although the theory may yield over- or underestimations when applied to a particular area of nearshore bottom current velocity. The potential errors are nevertheless within an acceptable range from an average

wave energy perspective. Regarding the bottom current velocity in nearshore surf zone approximated sawtooth waves, to simplify the problem, this study applied [11] sawtooth theory for the bottom current velocity analysis. To describe the asymmetry parameter (S_k) of the trajectory velocity $u_w(t)$ regarding sawtooth waves, comparison were made in relation to breaker indices, as shown in Fig. 4.

TABLE I: INPUT CONDITIONS

Simulation slope							
1/20		1/40		1/60			
Input wave height, H0							
0.5	1.0	1.5	2.0	2.5	3.0		
Input period, T0							
5	6	7	8	9	10	11	12

TABLE II: BREAKER TYPES

Breaker Type	ξ_0	ξ_b
Spilling	$\xi_0 < 0.46$	$\xi_b < 0.4$
Plunging	$0.46 < \xi_0 < 3.3$	$0.4 < \xi_b < 2.0$
Surging	$\xi_0 > 3.3$	$\xi_b > 2.0$

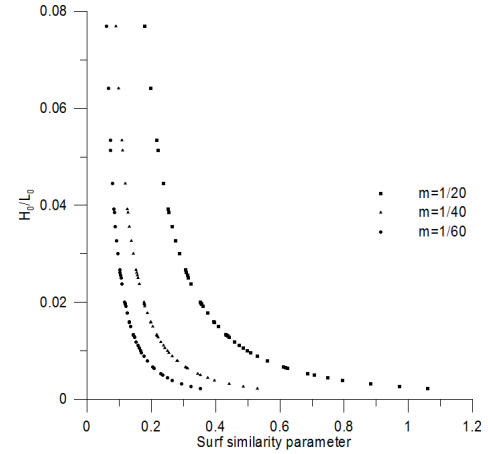


Fig. 3. Comparison of surf similarity parameters and breaker indices.

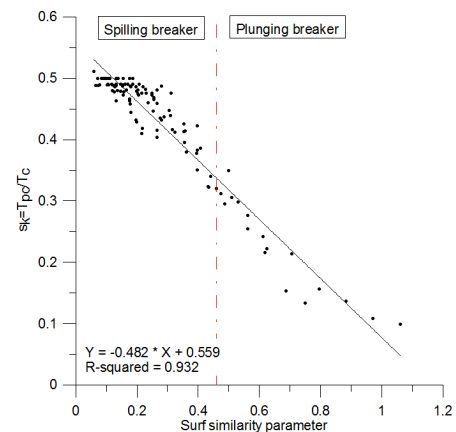


Fig. 4. Comparison of surf asymmetry parameters and surf similarity parameters.

Indicated by Fig. 4, the input conditions in effect under consideration slope, used in this study include spilling breaker and plunging breaker. And the distribution of the overall trend is that when the surf similarity parameter is larger, the smaller asymmetrical parameter:

$$s_k = -0.482\xi_0 + 0.559 \quad (32)$$

By substituting Eq. (31) into Eq. (32), the slope parameter of the parties within the surf zone of coastal waters is described by the sawtooth:

$$m\left(\frac{H_0}{L_0}\right)^2 s_k - 0.559\left(\frac{H_0}{L_0}\right)^2 + 0.482 = 0 \quad (33)$$

On the basis of the aforementioned assumption that the current velocity sequence in the surf zone is described regarding sawtooth waves, the determination of the surf asymmetry parameters may facilitate the resolution of the root mean square velocity within the surf zone, and the equivalent current velocity of the wave crest and trough half-cycle in the moving direction. Furthermore, characteristics that are computationally convenient with acceptable errors can be applied.

V. CONCLUSION

This study investigated the asymmetry parameters of bottom current velocity on the basis of the stokes 2nd theory, which, although susceptible to over- or underestimation when applied to general coastal areas, yields an average error derived from wave energy that is nevertheless within an acceptable range. The current velocity of the bottom coastal waters within the surf zone was computed with the sawtooth wave theory because of its computational convenience and acceptable error range. From the perspective of wave steepness or water depth variances, a trend was observed that the greater the breaker similarity parameters were, the smaller the surf asymmetry parameters became. The application scope and accuracy of the results may be further improved if other theories or numerical analyses such as the equivalent shear stress and bed friction could be considered in future studies.

REFERENCES

- [1] R. L. Wiegel, *Oceanographical Engineering*, Prentice-Hall, Inc., New Jersey, 1964.
- [2] H. W. Iversen, "Waves and breakers in shoaling water," in *Proc. 3rd Conf. Coastal Eng.*, ASCE, pp. 1-12, 1952.
- [3] Y. Goda, "Irregular wave deformation in the surf zone," *Coastal Eng. In Japan*, vol. 19, pp. 13-26, 1975.
- [4] D. W. Ostendorf and O. S. Madsen, "An analysis of longshore currents and associated sediment transport in the surf zone," *MIT Rep.*, Sea Grant 79-13, p. 169, 1979.
- [5] T. Sunamura, "Determination of breaker height and depth in the field," *Ann. Rep.*, Inst. Geosci., Univ. Tsukuba, no. 8, pp. 53-54, 1983.

- [6] B. L. ÉM haut éand R. C. Y. Koh, "On the breaking of waves arriving at an angle to the shore," *J. Hydraul. Res.*, vol. 5, no. 1, pp. 67-88, 1976.
- [7] M. Dibajnia and A. Watanabe, "Sheet flow under non-linear waves and currents," in *Proc. 23rd Int. Conf. on Coastal Eng.*, pp. 2015-2028, 1992.
- [8] M. Dibajnia and A. Watanabe, "A representative wave model for estimation of nearshore local transport rate," *Coastal Eng. In Japan*, vol. 43, no. 1, pp. 1-38, 2001.
- [9] R. L. Soulsby, *Dynamics of Marine Sands*, Thomas Telford Publications, London, 1997.
- [10] R. G. Dean and R. A. Dalrymple, *Water Wave Mechanics for Engineers and Scientists*, Prentice-Hall, Inc., New Jersey, 1984.
- [11] A. Watanabe and S. Sato, "A sheet-flow transport rate formula for asymmetric, forward-leaning waves and currents," in *Proc. 29th Int. Conf. on Coastal Eng.*, pp. 1703-1714, 2004.
- [12] J. A. Battjes, Surf Similarity, in *Proc. 14th Conf. Coastal Eng., ASCE*, pp. 466-480, 1974.



Yun-Chih Chiang received the Ph.D. degree in 2009, at the Department of Engineering Science and Ocean Engineering, National Taiwan University. Currently in the Center for General Education (Tzu Chi University, Taiwan) as an associate professor.

His research interests include coastal engineering, sediment transport, topography changes, nearshore hydrodynamics and the ocean renewable energy.



Sung-Shan Hsiao is a professor at the Department of Harbor and River Engineering, National Taiwan Ocean University, and taught for nearly three decades. Our goal is to educate students to become both a theoretical and practical engineers. And aims to engage with the major national construction and development of marine science and technology.

His research interests and expertise are about sediment transport, oceanographic measurements, nearshore hydrodynamics and coastal environment management.



Hui-Ming Fang received the Ph.D. degree in 2008, at the Department of Harbor and River Engineering, National Taiwan Ocean University. Currently in the same university as an assistant professor.

His research interests include ocean engineering, oceanographic measurements, coastal protection, disaster prevention and management, and cloud computing.



Hsing-Yu Wang received the master degree in 2009, the Department of Harbor and River Engineering, National Taiwan Ocean University. And he continued to a doctorate, now is a Ph.D. candidate.

His learning interests and expertise are coastal engineering, sediment transport, topography changes, oceanographic measurements and coastal environment management.